A Metastasis Modifier Locus on Human Chromosome 8p in Uveal Melanoma Identified by Integrative Genomic Analysis

Michael D. Onken, Lori A. Worley, and J. William Harbour

Abstract

Purpose: To identify genes that modify metastatic risk in uveal melanoma, a type of cancer that is valuable for studying metastasis because of its remarkably consistent metastatic pattern and well-characterized gene expression signature associated with metastasis.

Experimental Design: We analyzed 53 primary uveal melanomas by gene expression profiling, array-based comparative genomic hybridization, array-based global DNA methylation profiling, and single nucleotide polymorphism–based detection of loss of heterozygosity to identify modifiers of metastatic risk. A candidate gene, leucine zipper tumor suppressor-1 (*LZTS1*), was examined for its effect on proliferation, migration, and motility in cultured uveal melanoma cells.

Results: In metastasizing primary uveal melanomas, deletion of chromosome 8p12-22 and DNA hypermethylation of the corresponding region of the retained hemizygous 8p allele were associated with more rapid metastasis. Among the 11 genes located within the deleted region, *LZTS1* was most strongly linked to rapid metastasis. *LZTS1* was silenced in rapidly metastasizing and metastatic uveal melanomas but not in slowly metastasizing and nonmetastasizing uveal melanomas. Forced expression of LZTS1 in metastasizing uveal melanoma cells inhibited their motility and invasion, whereas depletion of LZTS1 increased their motility.

Conclusions: We have described a metastatic modifier locus on chromosome 8p and identified *LZTS1* as a potential metastasis suppressor within this region. This study shows the utility of integrative genomic methods for identifying modifiers of metastatic risk in human cancers and may suggest new therapeutic targets in metastasizing tumor cells.

Metastasis is the leading cause of death in cancer patients. However, the genetic mechanisms governing metastasis remain poorly understood. Indeed, dozens of oncogenes and tumor suppressor genes involved in early tumorigenesis have been characterized, but only about 10 metastasis suppressor genes have been identified (1). The search for new metastasis modifier loci has been hampered by the enormous complexity of the metastatic process, involving local invasion, entry into the circulation or lymphatic system, survival from hemodynamic shear stresses in the circulation, evasion of the immune system, and then extravasation, migration, proliferation, and recruitment of a blood supply at the metastatic site (2). Consequently, genetic modifiers of metastasis have been studied mostly in model organisms (1, 3). Our goal is to identify such modifiers in human cancers through whole-genome analytical techniques.

Uveal melanoma is valuable for studying modifiers of metastatic efficiency in a human cancer. Metastasis occurs in about half of these cancers and is uniformly fatal within a few months (4). Because of the anatomic constraints of the eye, uveal melanoma does not spread by local invasion or lymphatic dissemination but exclusively by the hematogenous route. Further, gene expression profiling of primary uveal melanomas has revealed two molecular classes, which are highly associated with clinical outcome (5). Tumors with the "class 1" signature have a very low risk of metastasis, whereas those with the "class 2" signature have a high risk of metastasis. The predictive accuracy of the class 2 signature is vastly superior to traditional clinical, pathologic, and cytogenetic risk factors (6). However, the time from diagnosis of the primary tumor to discovery of metastasis can range from less than a month to several decades (7, 8), and the class 2 signature does not distinguish between slowly and rapidly metastasizing tumors.

In this study, we analyzed 53 primary uveal melanomas by gene expression profiling, array-based comparative genomic hybridization, array-based global DNA methylation profiling, and single nucleotide polymorphism (SNP)–based detection of loss of heterozygosity. The only genetic variable that modified the predictive information of the class 2 signature was deletion of chromosome 8p, which was associated with more rapid onset of metastasis. Integrative genomic analysis revealed a minimal deleted region on 8p that corresponded to a genomic neighborhood that underwent DNA hypermethylation on the retained allele. One of the genes in this region was the

Authors' Affiliation: Department of Ophthalmology and Visual Sciences, Washington University School of Medicine, St. Louis, Missouri

leucine zipper tumor suppressor-1 (*LZTS1*), which was silenced in rapidly metastasizing and metastatic tumor cells but not in slowly metastasizing and nonmetastasizing tumor cells. Depletion of LZTS1 caused an increase in motility and invasion of metastasizing tumor cells. These results identify a region on chromosome 8p that modifies metastatic efficiency, suggest a role for *LZTS1* as a metastasis suppressor, and show the utility of integrative genomic methods for identifying genetic modifiers of metastatic risk in human cancers.

Materials and Methods

Tumor samples. This study was approved by the Human Studies Committee at Washington University, and informed consent was obtained from each subject. Uveal melanoma samples included in the study were treated by enucleation. Exclusion criteria included advanced/neglected local disease (one patient) and marked RNA degradation from tumor necrosis (one patient). Immediately after enucleation, the eye was opened to obtain tumor tissue that was snap frozen and prepared for RNA and DNA analysis as described previously (5). Uveal melanoma metastases were collected from liver biopsies at the time of metastatic diagnosis. All samples were histopathologically verified. Clinical, pathologic, and molecular findings are summarized in Supplementary Table S1. Cytologic severity was ranked from lowest to highest based on relative content of spindle and epithelioid cells in a cohort of 45 tumors in a previously published study (9). Mean nucleolar size was quantitated in 25 cases using ImageJ software as described previously (10). These same 25 tumors were scored for mitotic rate by counting mitotic figures in 10 fields (×40).

Array-based comparative genomic hybridization. Array-based comparative genomic hybridization data were available from a previous study on 44 of the tumors listed in Supplementary Table S1 (6). Previously published samples were analyzed by either the Microarray Shared Resource at the Comprehensive Cancer Center, University of California-San Francisco, using a microarray-based platform containing a genome-wide collection of genomic contigs, or the Microarray and Genomics Facility of the Roswell Park Cancer Institute, using an array platform containing ∼6,000 BAC clones (5, 11). For this study, both arms of each autosomal chromosome were scored for loss or gain based on $\log_2$ mean raw ratio. A $\log_2$ mean raw ratio < -0.5 for at least 30% of probes on a chromosomal arm was scored as "loss" and $\log_2$ mean raw ratio > 0.5 for at least 30% of probes was scored as "gain."

Cytogenetic analysis of published cases. A literature review of cytogenetic analysis results in 336 published uveal melanomas yielded 169 cases that were informative for chromosomes 3 and 8. Each chromosomal arm was scored as loss, normal, or gain. A more detailed analysis, along with references, has been published in a separate article (12).

Gene expression profiling. Gene expression profiling was done on one or more of the following microarray platforms: Affymetrix U133A GeneChip (28 cases), U133Av2 GeneChip (11 cases), and Illumina Ref8 Beadchip array (26 cases). Analysis of these profiles has been published elsewhere (5, 6, 9). For this study, new analyses were done on the 26 tumors evaluated on the Illumina Ref8 array. Raw expression data were subjected to rank invariant normalization and log transformation. Genes were filtered for a significance level of $P \leq 0.001$, which resulted in 829 genes for further analysis. Principal component analysis was done using Spotfire DecisionSite software version 8.2.1.[1] Hierarchical clustering was done using dChip software. For dChip analysis, rows were standardized by subtracting the mean and dividing by the SD, the distance metric was 1-Pearson correlation, the linkage method was centroid, and significant enrichment for genes on the same chromosome were determined using the dChip algorithm. Further details are available at the dChip Web site.[2] Validation of LZTS1 mRNA expression was done using the 7900HT

Real-Time PCR System (Applied Biosystems) with Applied Biosystems TaqMan Gene Expression Assays and primers (glyceraldehyde-3-phosphate dehydrogenase, Hs00266705_g1; LZTS1, Hs00232762_m1) following manufacturer's protocols.

SNP analysis. Twelve SNPs where chosen at approximate intervals of 6 ± 0.5 Mb across the euchromatic regions of chromosome 8p. SNPs were selected from the Ensembl *Homo sapiens* SNP database and were required to have a minor allele frequency >0.4 in the European population (which describes all patients in the study). This minor allele frequency allowed loss of heterozygosity to be inferred from tumor DNA without matching normal DNA at a significance level of $P < 0.52^n$ for n consecutive informative homozygous SNPs. This assumption was validated in a preliminary analysis of eight matching tumor and normal peripheral blood DNA samples of known genotype (data not shown). The SNPs selected for this study were rs2909619, rs4875237, rs20530, rs2062045, rs2517010, rs4921712, rs310325, rs1584233, rs4147357, rs1440530, rs4739456, and rs2923411. Sequenom SPECTRODESIGNER "IPLEX" software was used for the design of primers to permit genotyping in multiplex fashion. SNP-mass spectrometry-genotyping (13) was done with matrix-assisted laser desorption/ionization time-of-flight mass spectrometry by the Division of Human Genetics Genotyping Core Facility using the Sequenom MassARRAY system.[3] Allele calls and confidence scores were made by Sequenom software. Only high confidence calls were included in the analysis.

Genomic DNA methylation analysis. The CpG methylated fractions of genomic DNA were isolated from six primary tumors (MM32, MM41, MM46, MM48, MM54, and MM74; for more information on these samples, see Supplementary Table S1) using the MBD affinity column method provided in the Promoter Methylation PCR kit (Panomics) and following the manufacturer's protocol. Isolated fractions and fragmented input samples were amplified by linker-mediated PCR following a previously published protocol (14). Amplified samples were subjected to agarose gel electrophoresis and tested on the Nanodrop-1000 spectrophotometer (Nanodrop Technologies) to confirm quality and quantity before being sent to the University Health Network Microarray Centre for labeling and hybridization to their HCGI12K-Human CpG 12K Array. Labeling, hybridization, posthybridization washing, and microarray analysis procedures can be found at the University Health Network Web site.[4] Validation of DNA hypermethylation around the *LZTS1* promoter was done as follows. Primary tumor genomic DNA was digested with the methylation-sensitive restriction endonuclease *Eag*I (New England Biolabs), which digests DNA only if it is not methylated. Because this enzyme recognizes sites within the *LZTS1* promoter, it can be used to determine the methylation status of these sites. PCR primers were designed to amplify the *LZTS1* promoter, such that amplicons were produced only if the promoter was methylated, thereby preventing digestion of the promoter region. The primer sequences were TGATGGAAGTGAGAGCAGAGAGAC (forward) and CTCTCTTTTTTCCAGAGCTGCTGAGC (reverse). The presence of amplified products on agarose gels was interpreted to indicate methylation of the restriction sites.

Genomic DNA sequencing. Genomic sequence of the *LZTS1* gene was obtained through the University of California-Santa Cruz Genome Browser. Primers were designed using Primer3 software to amplify all coding regions as well as exon-intron boundaries. PCR amplicons were sequenced by the Washington University Genome Sequencing Center, and sequences were analyzed for polymorphisms and mutations using Sequencher 4.5 software (GeneCodes).

Cell culture assays. Mel202, Mel270, and 92.1 are human uveal melanoma cell lines derived from three different primary uveal melanomas that resulted in metastatic death (15–17).[5] None of these lines have 8p loss (18), and Mel202 has loss of heterozygosity for chromosome 3 (19). All cell lines were grown in RPMI 1640 (Lonza)

---

[1] http://www.spotfire.com

[2] http://biosun1.harvard.edu/complab/dchip/

[3] http://hg.wustl.edu/info/Sequenom.description.html
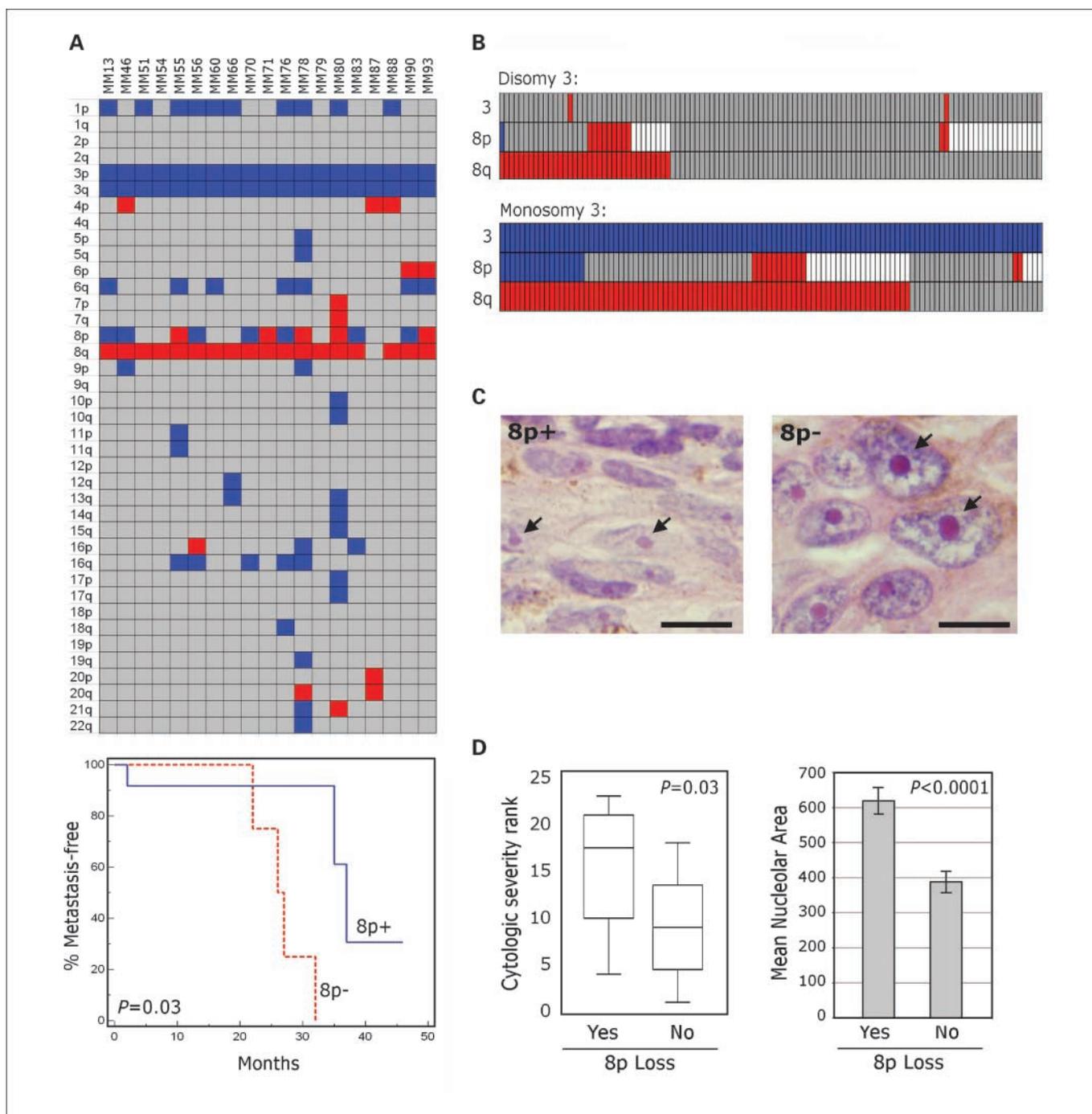
[4] http://www.microarrays.ca/

Fig. 1. Loss of 8p in primary uveal melanomas is associated with aggressive morphology and rapid metastasis. *A, top,* heat map of array-based comparative genomic hybridization results showing status of the indicated chromosomal arms in 19 primary tumors with the metastasizing class 2 gene expression signature (red, gain; blue, loss; gray, no change). *Bottom,* survival analysis in patients with class 2 tumors, stratified by 8p status, using the Kaplan-Meier method. *B,* heat map of published cytogenetic findings in 169 primary uveal melanomas (*red,* gain; *blue,* loss; *gray,* no change; *white,* not reported). *C,* histologic sections stained with H&E from representative class 2 tumors without (*left*) and with (*right*) 8p loss (*arrows,* nucleoli). *D,* graphs showing association between 8p loss and cytologic severity in 45 tumors (*left*) and nucleolar area in 25 tumors (*right*). *Left,* box-and-whiskers plot; *central box,* values from the lower to upper quartile (25-75 percentile); *middle line,* median; *vertical line,* from the minimum to the maximum value.

supplemented with 10% fetal bovine serum (Invitrogen) and antibiotics. Transfections were done using Effectene (Qiagen) with the following: Hs_LZTS1_1_HP and Hs_LZTS1_3_HP (50:50) small interfering RNA (Qiagen) or a scrambled control small interfering RNA (Qiagen),

pExpress1-LZTS1 (Invitrogen), or empty pCMV-neo control, and cotransfected with pCMS-EGFP (10:1 ratio; BD Biosciences). Changes in LZTS1 expression were confirmed by Western blot using antibodies that recognize the LZTS1 protein (Santa Cruz Biotechnology) and α-tubulin (Sigma-Aldrich; Supplementary Fig. S1). After 24 h, transfected cells were trypsinized and plated into 8-well Lab-Tek Permanox Chamber Slides (Nunc) for motility and cell growth assays and into the upper
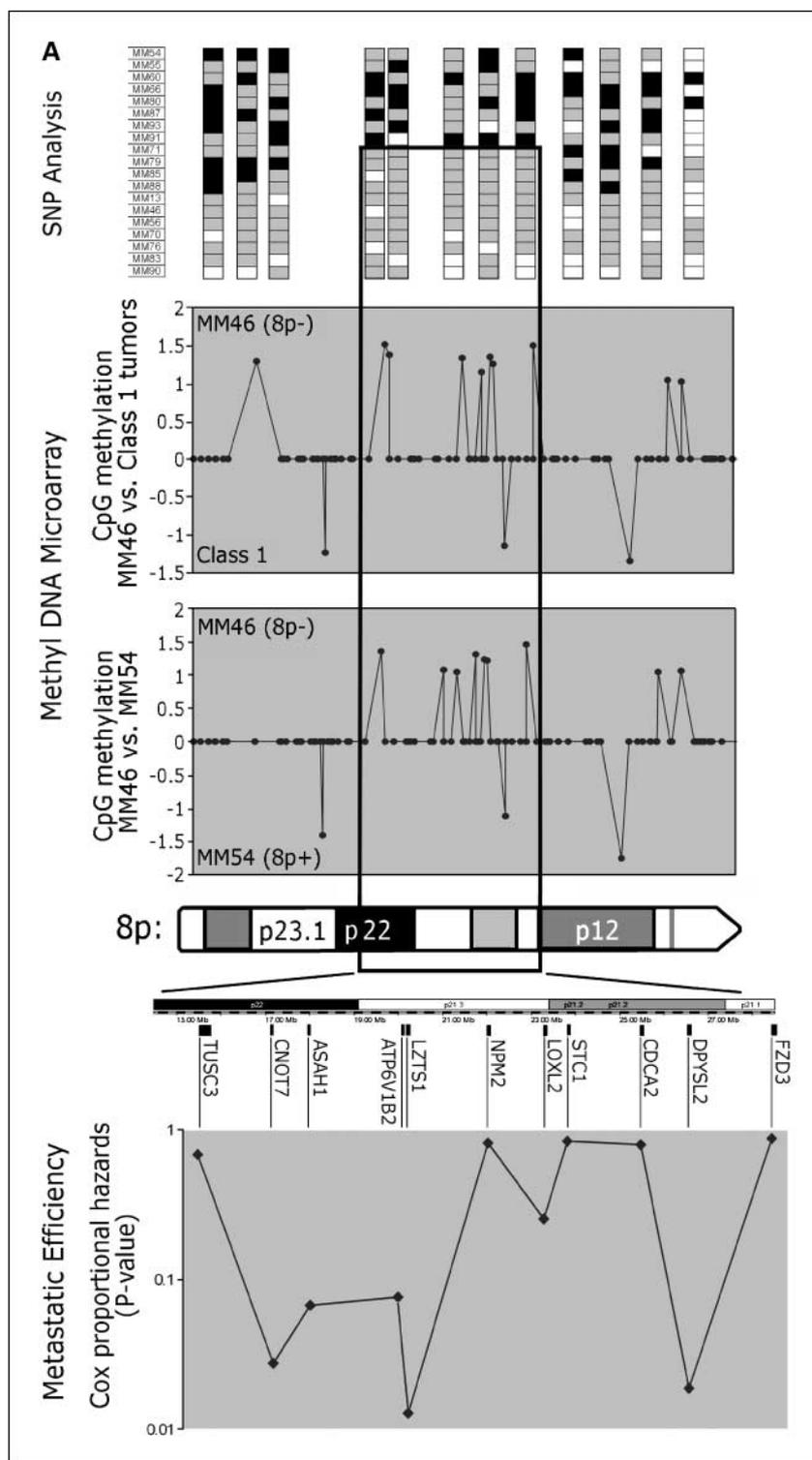
Fig. 2. A region of DNA deletion and hypermethylation on chromosome 8p in rapidly metastasizing uveal melanomas. *A, top,* SNP analysis of class 2 tumors identifies a minimally deleted region; *middle,* minimal deleted region corresponds to a region of DNA hypermethylation (identified by array based profiling of methylated CpG islands) on the retained, hemizygous allele in rapidly metastasizing class 2B tumors; *bottom,* genes located within the minimally deleted region and their association with metastatic efficiency based on Cox proportional hazards analysis of gene expression versus time to metastasis.

chambers of 12-well Transwell plates (Corning) for cell invasion assays. Motility assays were carried out as described previously (20). Transfection rates varied from 20% to 40% among cell lines. To correct for differences in transfection efficiency, only cells that were positive for green fluorescent protein expression were scored. Efficient transfection was very low for small interfering RNA in the 92.1 cell line, so this was not included in the study. For cell invasion assays, cells were suspended in growth medium without serum and placed in the upper chambers of Transwell membrane supports that had been coated with bovine type I

collagen (Sigma-Aldrich) the day before. After 18 h, media were removed and the upper faces of the membranes were gently cleaned with cotton swabs to remove cells. The membranes were then removed from their supports and placed face up on glass slides and coverslipped under PBS. Total green fluorescent protein–positive cells were scored for each membrane under fluorescent microscopy.

Statistical analysis. All statistical calculations were done using MedCalc software version 9.3.6.0. Time-dependent analysis was done using the Cox proportional hazards method for continuous variables
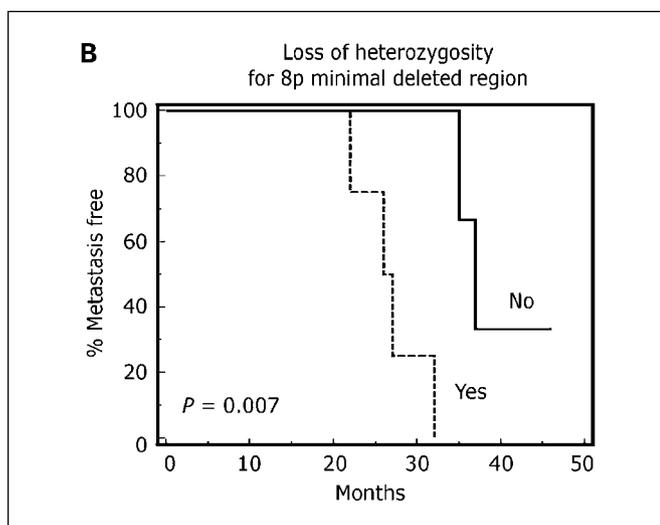
Fig. 2 *Continued. B,* Kaplan-Meier survival analysis of time to metastasis based on the presence or absence of DNA loss within the minimally deleted region on 8p.

and the Kaplan-Meier method for discontinuous variables. For Cox proportional hazards analysis of the 11 genes on 8p, expression values were converted to nonparametric rank data to allow Affymetrix and Illumina data to be combined.

Results

Chromosomal analysis. Fifty-three primary uveal melanomas were assigned to the low-risk class 1 group (28 tumors) or the high-risk class 2 group (25 tumors) by gene expression profiling as described previously (5, 6). At the time of the study, metastasis had occurred in 10 of the class 2 tumors at a median time of 27 months from primary tumor diagnosis (range, 14-45 months). No clinical features modified the risk of metastasis. Chromosomal copy number changes were assessed by array-based comparative genomic hybridization in 19 of the class 2 tumors (Fig. 1A). Besides chromosome 3 loss (all 19 tumors), frequent abnormalities included 8q gain (18 tumors), 1p loss (10 tumors), 8p loss (7 tumors), 6q loss (7 tumors), 16q loss (5 tumors), and 8p gain (5 tumors). Association between chromosomal alterations and time to metastasis was assessed by Cox proportional hazards for each chromosome arm. The only alteration that correlated with time to metastasis was 8p loss (P = 0.01). Interestingly, all tumors that exhibited 8p loss also showed 8q gain, consistent with isochromosome 8q (21). To confirm this association of isochromosome 8q with the class 2 signature, we conducted an overview of cytogenetic features in published uveal melanoma samples using monosomy 3 as a surrogate marker for the class 2 signature. Of 169 cases informative for both chromosomes 3 and 8, 8p loss was only observed in the context of 8q gain, and this alteration was observed in 17 of 85 (20%) monosomy 3 tumors compared with 1 of 84 (1.2%) disomy 3 tumors (Fisher's exact test, P = 7 × 10^{-5}; Fig. 1B). Phenotypically, 8p loss was associated with increased cytologic severity (P = 0.03) and nucleolar size (P < 0.0001; Fig. 1C and D), both of which have been linked to poor outcome (22), suggesting a functional link between one or more genes on 8p and tumor progression.

Interstitial deletion and DNA methylation on chromosome 8p. To further define the minimal deleted region on 8p, highly

polymorphic SNPs distributed across chromosome 8p were interrogated for loss of heterozygosity in the class 2 tumors (Fig. 2A). Seven tumors exhibited homozygosity at all informative loci, consistent with loss of the entire chromosomal arm. Four other tumors exhibited homozygosity of ≥5 consecutive internal loci, consistent with an interstitial 8p deletion (P ≤ 0.04). The minimal deleted region consisted of a 10 Mb stretch from 8p22 to 8p12. Loss of heterozygosity for the deleted region was even more strongly associated with rapid metastasis (Kaplan-Meier, P = 0.007) than was 8p loss by array-based comparative genomic hybridization (Fig. 2B). No homozygous deletions were identified. To investigate DNA methylation as a potential mechanism for transcriptional inactivation, DNA samples from six tumors (MM32, MM41, MM46, MM48, MM54, and MM74) were interrogated using methyl-DNA-binding columns followed by hybridization of the enriched samples to the HCGI12K-Human CpG 12K Array. Because these methylation analyses are expensive and time intensive and require a significant input of fresh DNA, it was impractical to do this on all cases. Rapidly metastasizing class 2B tumor cells exhibited a region on 8p that was hypermethylated relative to the slowly metastasizing class 2A and nonmetastasizing class 1 tumor cells (Fig. 2A). This methylated region overlapped the minimal deleted region identified by SNP analysis.

Gene expression profiling. As an independent method for identifying genetic modifiers of metastatic risk, we analyzed gene expression profiles from 14 class 1 and 12 class 2 tumors that were investigated on the Illumina BeadChip array. Using principal component analysis as an unsupervised analysis, the tumors segregated into two major clusters, corresponding to the class 1 and class 2 signatures (Fig. 3A). The class 2 tumors further segregated into two subclusters, hereafter referred to as class 2A and class 2B. Class 2B tumors were associated with more rapid onset of metastasis than class 2A tumors (Fig. 3B). Hierarchical clustering of class 2A and 2B tumors using the dChip algorithm identified a highly significant cluster of 17 genes on 8p that were down-regulated in subclass 2B (P < 10^{-7}; Fig. 3C). Thus, gene expression profiling and the chromosomal analysis both implicated genetic inactivation on 8p as a modifier of metastatic risk. Eleven well-defined genes were located within the deleted region identified by SNP, and six of these (*CNOT7*, *ASAH1*, *ATP6V1B2*, *LZTS1*, *DPYSL2*, and *FZD3*) were down-regulated in the subclass 2B signature. Of these six, *LZTS1* was most strongly linked to rapid metastasis (P = 0.01) by Cox proportional hazards (Fig. 2A).

Analysis of LZTS1. LZTS1 mRNA expression was down-regulated in rapidly metastasizing class 2B tumors and metastatic tumor cells relative to slowly metastasizing class 2A tumors by microarray analysis (Fig. 4A) and by quantitative PCR (Fig. 4B). The significance of correlation between array-based and PCR-based LZTS1 expression was P = 0.05. Exons and flanking sequences of the *LZTS1* gene were interrogated by direct sequencing in seven class 2B tumors, but no mutations were identified (data not shown). Nevertheless, the *LZTS1* promoter on the retained hemizygous allele showed a higher degree of methylation in class 2B tumors compared with class 1 and class 2A tumors (Fig. 4C). The effect of LZTS1 on mitotic rate was analyzed by counting mitotic figures per high-power field in primary tumor sections stained with H&E in class 2A and class 2B tumors. The median number of mitotic figures was greater in class 2B tumors, although this difference was not
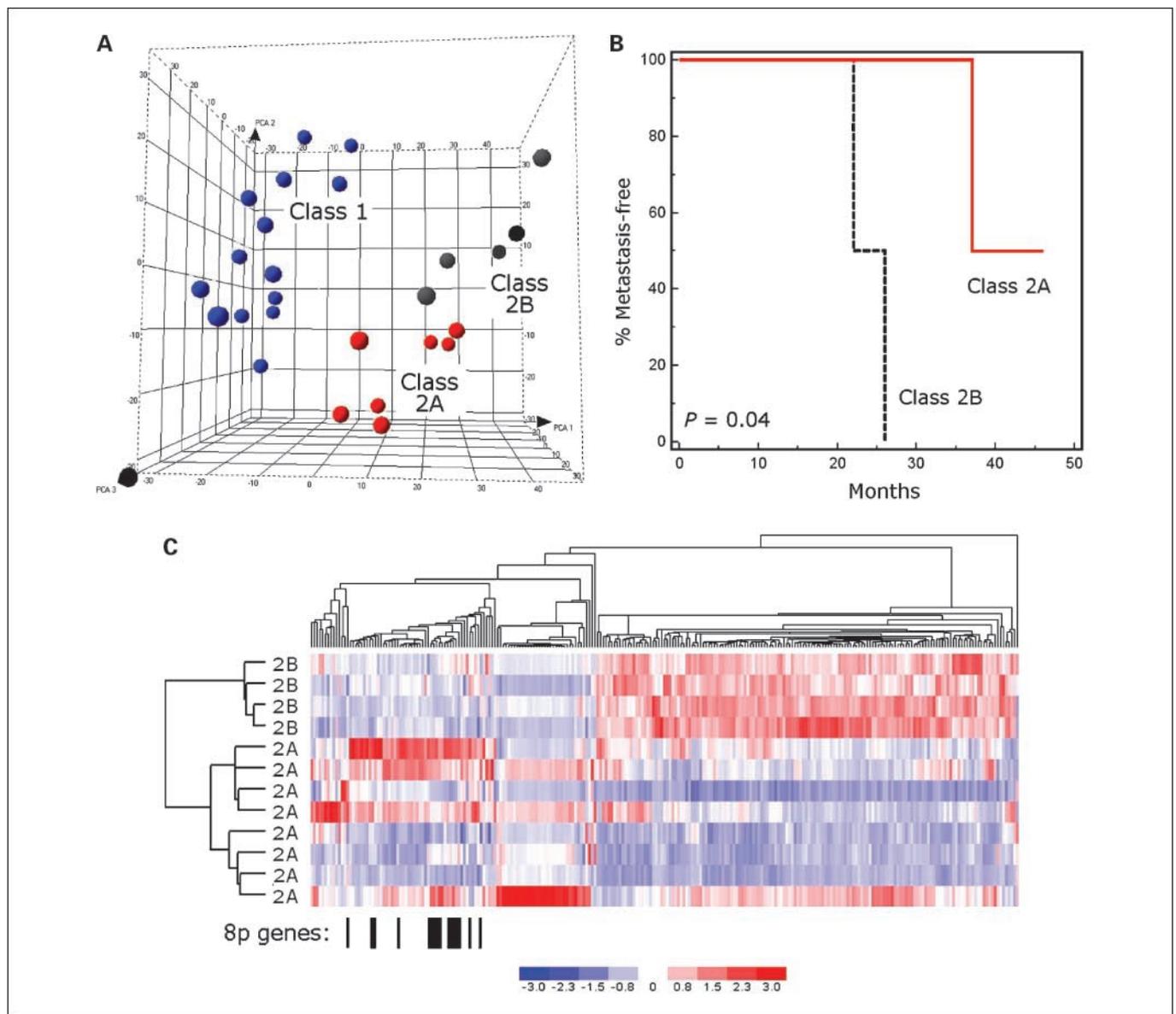
Fig. 3. Gene expression profiling identifies two subclasses of metastasizing class 2 uveal melanomas. *A,* principal component analysis of 26 primary tumors showing the first three principal components and the clustering of tumors into class 1 (*blue spheres*), class 2A (*red spheres*), and class 2B (*black spheres*). *B,* Kaplan-Meier survival analysis of class 2A versus class 2B tumors. *C,* hierarchical clustering of tumors into subgroups 2A and 2B, with a significant overrepresentation of 8p genes among those that were down-regulated in the class 2B tumors.

significant (P = 0.62; Fig. 4D). To investigate the role of LZTS1 in acquisition of the metastatic phenotype, we analyzed the effects of LZTS1 overexpression and depletion in metastasizing uveal melanoma cells. Uveal melanoma cells overexpressing LZTS1 exhibited decreased invasion and motility (Fig. 5A-C). Conversely, uveal melanoma cells depleted of LZTS1 using small interfering RNA exhibited increased motility (Fig. 5B and C). Modulation of LZTS1 mRNA levels did not alter the proliferation rate in these cells (Fig. 4D).

Discussion

Most current anticancer agents inhibit specific oncoproteins that are mutated in the primary tumor (23), or they have nonspecific mechanisms of action and are used mainly to treat metastatic disease. Few existing agents are designed to prevent or delay the onset of metastatic disease, which could have a profound public health effect in a disease population composed mostly of older individuals. This deficit in our therapeutic armamentarium is due in large part to incomplete understanding of the molecular events regulating metastasis. This study shows that integrative genomic methods can be used in human cancers to identify molecular modifiers of metastatic efficiency that could be therapeutically targeted.

In primary uveal melanomas with the highly metastatic class 2 signature, deletion of the region 8p12-22 was associated with a more rapid onset of metastasis, indicative of increased metastatic efficiency. This deleted region overlapped a region that had been shown previously to suppress metastasis in a rat prostate cancer model using microcell-mediated

chromosome transfer (24). The corresponding region of the retained, hemizygous chromosomal arm exhibited a "neighborhood" pattern of DNA hypermethylation and transcriptional silencing, consistent with recent work showing that such epigenetic alterations may occur by instructive, rather than random, mechanisms (25, 26). There were three potential metastasis suppress genes within this region: *CNOT7*, *DPYSL2*, and *LZTS1*. Each of these was differentially expressed in the subclass 2B tumors and associated with shorter time to metastasis. Previous studies of *CNOT7* did not find tumor suppressor activity (27). *DPYSL2* is involved in axon guidance but has not been linked to cancer (28). Thus, we focused initially on *LZTS1*, which was most strongly linked to time to metastasis and has been shown to be a tumor suppressor (29).

LZTS1 encodes a leucine zipper-containing protein that is inactivated in multiple cancer types (29, 30), but our findings implicate *LZTS1* specifically as a potential modifier of metastatic efficiency. *LZTS1* is located within the minimally deleted region that was reduced to homozygosity in rapidly metastasizing tumors. The *LZTS1* promoter was hypermethy-

lated and silenced in rapidly metastasizing tumor cells but not in slowly metastasizing and nonmetastasizing tumor cells. In addition, *LZTS1* had the highest predictive value of any gene on 8p and lies within a hypermethylated locus in the minimal deleted region of 8p. Further, LZTS1 exhibited down-regulation in lymph node and visceral metastases from cutaneous melanomas in a published database (Supplementary Fig. S2; ref. 31). Unfortunately, no class 2B derived cell lines could be identified, so demethylation of 8p using agents such as 5-azacytidine could not be done. The ability of LZTS1 to suppress motility and invasion in uveal melanoma cells shows that silencing *LZTS1* through deletion of one allele and hypermethylation of the other allele could promote metastasis by enhancing the ability of tumor cells to migrate and intravasate into the circulation. Because LZTS1 has been shown to function, at least in part, as a mitotic regulator (32), it was surprising that LZTS1 did not appear to affect mitotic rate but rather motility and invasion. However, these are typical characteristics of the metastasis suppressor genes (1), and perhaps the function of LZTS1 is different in different cell types.
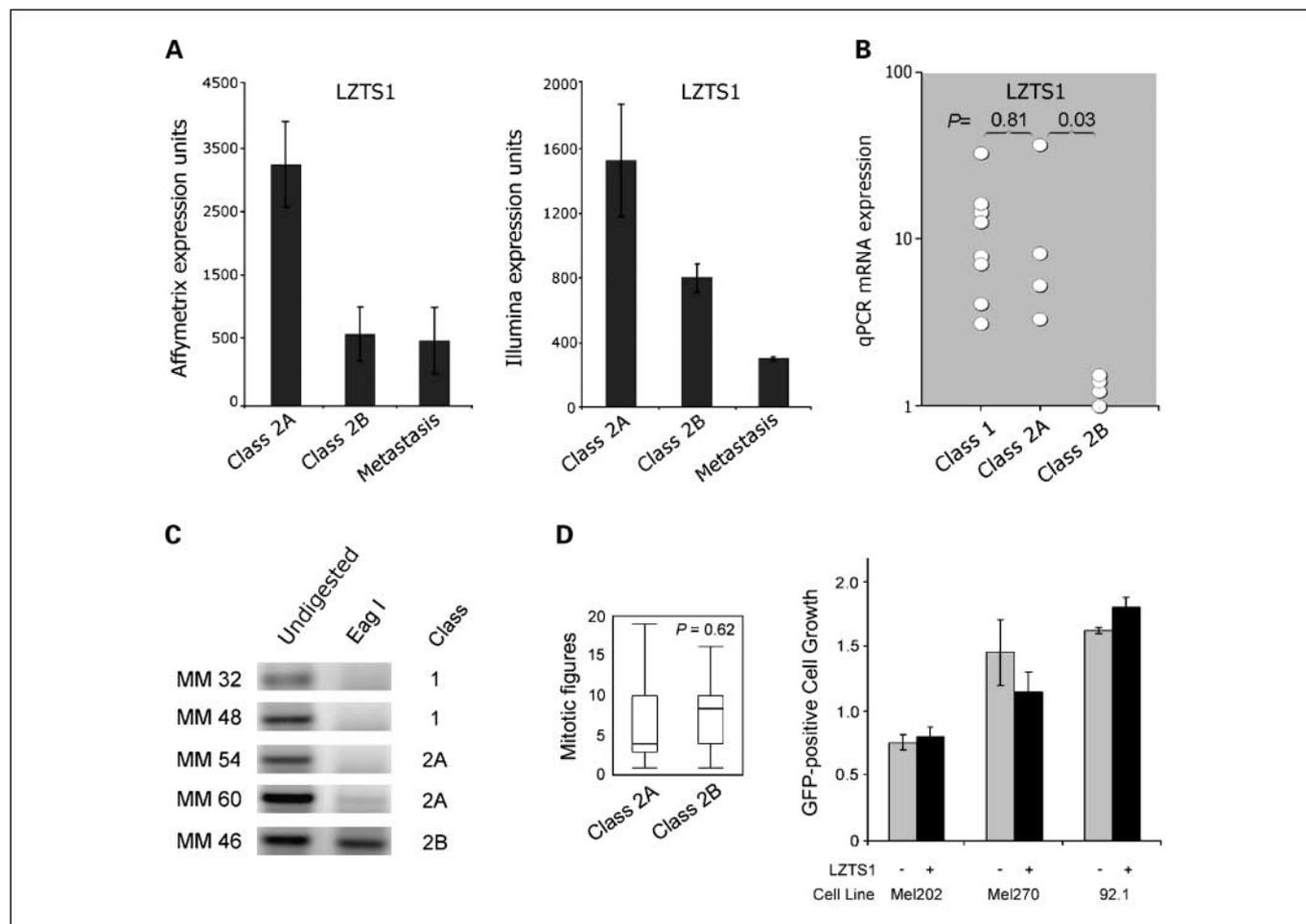

Fig. 4. The *LZTS1* promoter is methylated and silenced in class 2B primary tumors and silenced in uveal melanoma metastases. *A,* LZTS1 mRNA expression in class 2A, class 2B, and metastatic tumor tissue based on Affymetrix U133A (*left*) and Illumina Ref8 (*right*) microarrays. *B,* LZTS1 mRNA expression in class 1, class 2A, and class 2B tumor tissue based on quantitative PCR. *C,* DNA methylation of the *LZTS1* promoter in class 1, class 2A, and class 2B tumor cells. Bands represent CpG islands amplicons that were not digested by the restriction enzyme *Eag* I, which only digests DNA that is unmethylated. Similar results were obtained with another methylation-sensitive restriction enzyme *Sac* II (data not shown). *D,* LZTS1 expression does not significantly affect proliferation rates *in vivo* or *in vitro*. *Left,* box-and-whiskers plot of mitotic figures per high-power field from class 2A and class 2B tumors; *right,* fold increase in the number of green fluorescent protein – positive cells at 4 days post-transfection relative to 1 day post-transfection for uveal melanoma cell lines transfected with control (*gray columns*) or LZTS1 (*black columns*) expression constructs.
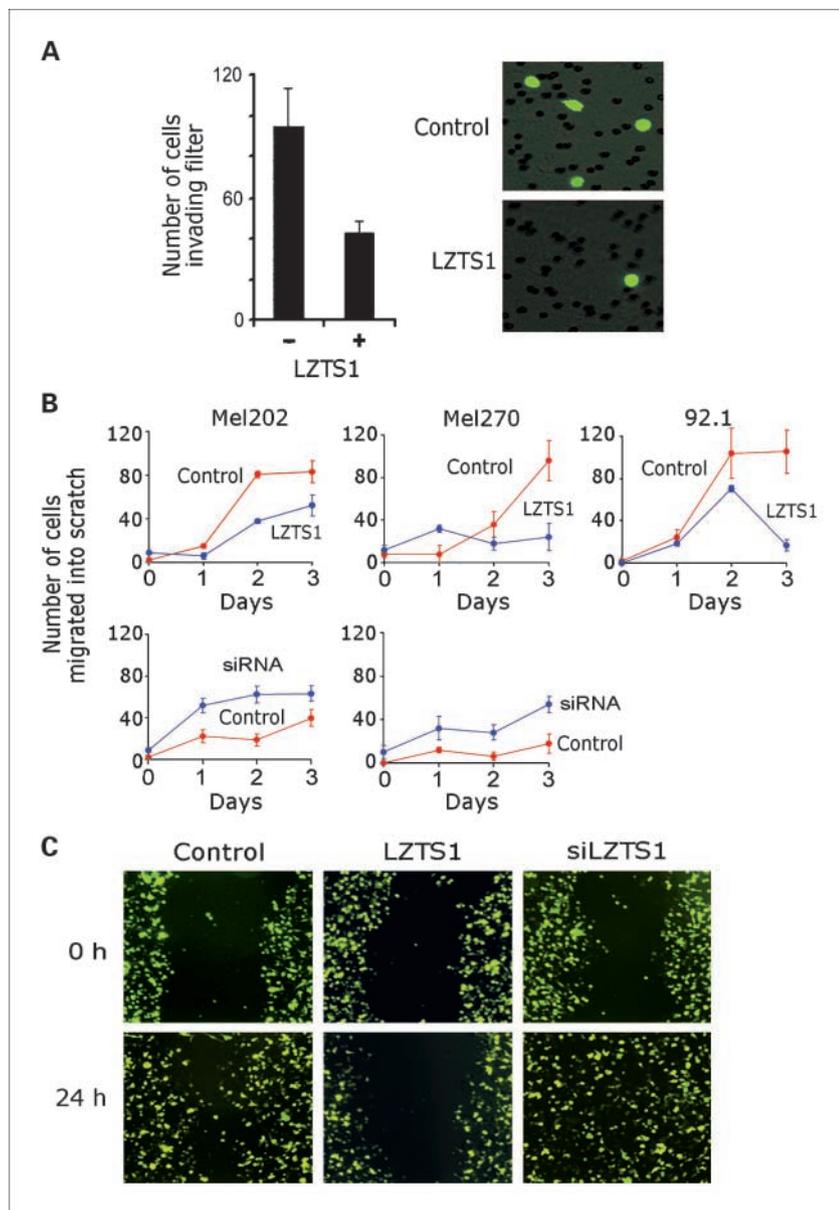
Fig. 5. LZTS1 inhibits motility and invasion in uveal melanoma cells. *A, left,* invasion assays showing effect of LZTS1 overexpression in metastasizing Mel202 tumor cells; *right,* representative fields from control and LZTS1-transfected cells. Only transfected cells, identified by green fluorescent protein, were counted. *B,* results of motility assays in three metastasizing tumor cell lines transfected with an LZTS1 expression vector, LZTS1 small interfering RNA, or the appropriate control. *Columns,* mean of three independent experiments; *bars,* SE. No significant differences were noted among replicate experiments. *C,* representative images of motility assays showing the ability of Mel202 cells transfected with the indicated vectors to migrate into a "wound" at time 0 and at 24 h. Only transfected cells, identified by green fluorescent protein, were counted.

Two critical events in uveal melanoma progression have now been identified. The earlier event is the development of the class 2 gene expression signature, which is usually accompanied by deletion of chromosome 3 (11). This event appears to be rate-limiting in the acquisition of metastatic competence: the class 1 signature resembles that of normal differentiated melanocytes, whereas the class 2 signature is enriched for genes expressed in neuroectodermal stem cells (9), suggesting that one or more genes on chromosome 3 may regulate the emergence of a cancer stem-like phenotype.[6] Here, we show that a second important event in metastatic progression is silencing of a region on 8p, which modifies the metastatic efficiency of class 2 tumor cells. This is consistent with our recent work showing that 8p loss is a late event in uveal melanoma progression (12).

These findings show the potential for personalized, preemptive treatment of cancer patients who are at high risk of metastasis based on genetic profiling of the primary tumor. They also indicate that integrative genomic methods can be used to identify novel targets for therapeutic intervention in the metastatic process. Consequently, traditional tumor classifications based on morphologic features such as size, location, and level of invasion will need to be modified to take into account this emerging molecular information. Toward this goal, we have initiated a prospective, multicenter study to evaluate the predictive value of the gene expression classifier and the 8p deletion in biopsy specimens from uveal melanoma patients.

Disclosure of Potential Conflicts of Interest

No potential conflicts of interest were disclosed.

Acknowledgments

---

[6] S.H. Chang, L.A. Worley, M.D. Onken, M.E. Smith, and J.W. Harbour, unpublished data.

References

1. Berger JC, Vander Griend DJ, Robinson VL, Hickson JA, Rinker-Schaeffer CW. Metastasis suppressor genes: from gene identification to protein function and regulation. Cancer Biol Ther 2005;4:805–12.

2. MacDonald IC, Groom AC, Chambers AF. Cancer spread and micrometastasis development: quantitative approaches for *in vivo* models. Bioessays 2002; 24:885–93.

3. Brumby AM, Richardson HE. Using *Drosophila melanogaster* to map human cancer pathways. Nat Rev Cancer 2005;5:626–39.

4. Harbour JW. Clinical overview of uveal melanoma: introduction to tumors of the eye. In: Albert DM, Polans A, editors. Ocular Oncology. New York: Marcel Dekker; 2003. p. 1–18.

5. Onken MD, Worley LA, Ehlers JP, Harbour JW. Gene expression profiling in uveal melanoma reveals two molecular classes and predicts metastatic death. Cancer Res 2004;64:7205–9.

6. Worley LA, Onken MD, Person E, et al. Transcriptomic versus chromosomal prognostic markers and clinical outcome in uveal melanoma. Clin Cancer Res 2007; 13:1466–71.

7. Coupland SE, Sidiki S, Clark BJ, McClaren K, Kyle P, Lee WR. Metastatic choroidal melanoma to the contralateral orbit 40 years after enucleation. Arch Ophthalmol 1996;114:751–6.

8. Sato T, Babazono A, Shields JA, Shields CL, De Potter P, Mastrangelo MJ. Time to systemic metastases in patients with posterior uveal melanoma. Cancer Invest 1997;15:98–105.

9. Onken MD, Ehlers JP, Worley LA, Makita J, Yokota Y, Harbour JW. Functional gene expression analysis uncovers phenotypic switch in aggressive uveal melanomas. Cancer Res 2006;66:4602–9.

10. Ehlers JP, Harbour JW. NBS1 expression as a prognostic marker in uveal melanoma. Clin Cancer Res 2005;11:1849–53.

11. Onken MD, Worley LA, Person E, Char DH, Bowcock AM, Harbour JW. Loss of heterozygosity of chromosome 3 detected with single nucleotide polymorphisms is superior to monosomy 3 for predicting metastasis in uveal melanoma. Clin Cancer Res 2007;13:2923–7.

12. Ehlers JP, Worley L, Onken MD, Harbour JW. Integrative genomic analysis of aneuploidy in uveal melanoma. Clin Cancer Res 2008;14:115–22.

13. Tai AL, Mak W, Ng PK, et al. High-throughput loss-of-heterozygosity study of chromosome 3p in lung cancer using single-nucleotide polymorphism markers. Cancer Res 2006;66:4133–8.

14. Oberley MJ, Tsao J, Yau P, Farnham PJ. High-throughput screening of chromatin immunoprecipitates using CpG-island microarrays. Methods Enzymol 2004;376:315–34.

15. Ksander BR, Rubsamen PE, Olsen KR, Cousins SW, Streilein JW. Studies of tumor-infiltrating lymphocytes from a human choroidal melanoma. Invest Ophthalmol Vis Sci 1991;32:3198–208.

16. Chen PW, Murray TG, Uno T, Salgaller ML, Reddy R, Ksander BR. Expression of MAGE genes in ocular melanoma during progression from primary to metastatic disease. Clin Exp Metastasis 1997;15:509–18.

17. Blom DJ, Schurmans LR, De Waard-Siebinga I, De Wolff-Rouendaal D, Keunen JE, Jager MJ. HLA expression in a primary uveal melanoma, its cell line, and four of its metastases. Br J Ophthalmol 1997;81:989–93.

18. Naus NC, Zuidervaart W, Rayman N, et al. Mutation analysis of the PTEN gene in uveal melanoma cell lines. Int J Cancer 2000;87:151–3.

19. Nareyeck G, Zeschnigk M, Prescher G, Lohmann DR, Anastassiou G. Establishment and characterization of two uveal melanoma cell lines derived from tumors with loss of one chromosome 3. Exp Eye Res 2006;83:858–64.

20. Ehlers JP, Worley L, Onken MD, Harbour JW. DDEF1 is located in an amplified region of chromosome 8q and is overexpressed in uveal melanoma. Clin Cancer Res 2005;11:3609–13.

21. Aalto Y, Eriksson L, Seregard S, Larsson O, Knuutila S. Concomitant loss of chromosome 3 and whole arm losses and gains of chromosome 1, 6, or 8 in metastasizing primary uveal melanoma. Invest Ophthalmol Vis Sci 2001;42:313–7.

22. Seddon JM, Polivogianis L, Hsieh CC, Albert DM, Gamel JW, Gragoudas ES. Death from uveal melanoma. Number of epithelioid cells and inverse SD of nucleolar area as prognostic factors. Arch Ophthalmol 1987;105:801–6.

23. Gollob JA, Wilhelm S, Carter C, Kelley SL. Role of Raf kinase in cancer: therapeutic potential of targeting the Raf/MEK/ERK signal transduction pathway. Semin Oncol 2006;33:392–406.

24. Nihei N, Kouprina N, Larionov V, et al. Functional evidence for a metastasis suppressor gene for rat prostate cancer within a 60-kilobase region on human chromosome 8p21-12. Cancer Res 2002;62: 367–70.

25. Frigola J, Song J, Stirzaker C, Hinshelwood RA, Peinado MA, Clark SJ. Epigenetic remodeling in colorectal cancer results in coordinate gene suppression across an entire chromosome band. Nat Genet 2006; 38:540–9.

26. Keshet I, Schlesinger Y, Farkash S, et al. Evidence for an instructive mechanism of *de novo* methylation in cancer cells. Nat Genet 2006;38:149–53.

27. Flanagan J, Healey S, Young J, Whitehall V, Chenevix-Trench G. Analysis of the transcription regulator, CNOT7, as a candidate chromosome 8 tumor suppressor gene in colorectal cancer. Int J Cancer 2003;106:505–9.

28. Fontan-Gabas L, Oliemuller E, Martinez-Irujo JJ, de Miguel C, Rouzaut A. All-*trans*-retinoic acid inhibits collapsin response mediator protein-2 transcriptional activity during SH-SY5Y neuroblastoma cell differentiation. FEBS J 2007;274:498–511.

29. Ishii H, Baffa R, Numata SI, et al. The FEZ1 gene at chromosome 8p22 encodes a leucine-zipper protein, and its expression is altered in multiple human tumors. Proc Natl Acad Sci U S A 1999;96:3928–33.

30. Ishii H, Vecchione A, Murakumo Y, et al. FEZ1/LZTS1 gene at 8p22 suppresses cancer cell growth and regulates mitosis. Proc Natl Acad Sci U S A 2001;98: 10374–9.

31. Smith AP, Hoek K, Becker D. Whole-genome expression profiling of the melanoma progression pathway reveals marked molecular differences between nevi/melanoma *in situ* and advanced-stage melanomas. Cancer Biol Ther 2005;4:1018–29.

32. Vecchione A, Baldassarre G, Ishii H, et al. Fez1/Lzts1 absence impairs Cdk1/Cdc25C interaction during mitosis and predisposes mice to cancer development. Cancer Cell 2007;11:275–89.

Clinical Cancer Research

A Metastasis Modifier Locus on Human Chromosome 8p in Uveal Melanoma Identified by Integrative Genomic Analysis

Michael D. Onken, Lori A. Worley and J. William Harbour

Updated version	Access the most recent version of this article at: http://clincancerres.aacrjournals.org/content/14/12/3737

Cited articles	This article cites 31 articles, 14 of which you can access for free at: http://clincancerres.aacrjournals.org/content/14/12/3737.full#ref-list-1
Citing articles	This article has been cited by 9 HighWire-hosted articles. Access the articles at: http://clincancerres.aacrjournals.org/content/14/12/3737.full#related-urls

E-mail alerts	Sign up to receive free email-alerts related to this article or journal.
Reprints and Subscriptions	To order reprints of this article or to subscribe to the journal, contact the AACR Publications Department at pubs@aacr.org.
Permissions	To request permission to re-use all or part of this article, use this link http://clincancerres.aacrjournals.org/content/14/12/3737. Click on "Request Permissions" which will take you to the Copyright Clearance Center's (CCC) Rightslink site.